2nd Intn'l Conf. on Hydroelasticity in Marine Technology, Fukuoka, Japan, 1-3 December 1998

Time-Domain Analysis of Ship Motions and Hydrodynamic Pressures on a Ship Hull in Waves

L. Z. Cong[1], Z. J.(Jerry) Huang[2], S. Ando[3] and C. C. Hsiung[1]

[1] *Centre for Marine Vessel Development and Research, DalTech, Dalhousie University, Halifax, Canada*
[2] *Mobil Technology Company, Dallas, Texas; Formerly with CMVDR, DalTech*
[3] *Defence Research Establishment Atlantic, Dartmouth, Nova Scotia, Canada*

ABSTRACT: This paper describes the development of a three-dimensional time-domain numerical model for calculating hull pressures as well as hydrodynamic forces for hydroelastic analysis of a ship hull in waves. In this work, hydrodynamic forces and pressures due to the radiated and diffracted waves are expressed as convolution products of a response function with either the velocity of ship motion or the wave elevation. The present method significantly reduces the need for numerical evaluation of the time-domain Green function in the convolution of memory effects. The response functions of forces and pressures of radiated and diffracted waves are obtained by numerically solving the Fredholm integral equation of the first kind. The present method to solve the integral equation directly in the time domain is much more robust than the widely used method based on the Fourier transformation, since the latter is fraught with numerical difficulties. In the equations of motion, maneuvering and rudder forces as well as the radiation and diffraction forces, nonlinear restoring and Froude-Krylov forces are taken into account.

1. INTRODUCTION

The time-domain hydrodynamic forces can be directly computed in the time domain or indirectly converted from the frequency-domain added masses and damping coefficients. Applications based on the frequency-domain hydrodynamic coefficients can be found in de Kat and Paulling's (1989) paper. In a more direct application of strip theory to the prediction of large-amplitude ship motions and loads in the time domain, the radiation and diffraction forces are calculated in terms of frequency-dependent sectional added-mass and damping coefficients. Either way, however, the strip-theory approach is inadequate for calculating hydrodynamic pressure distributions on the hull, which are necessary for structural analyses concerning grillages, panels, and plates, and the three-dimensional method must be used.

Based on the methods introduced by Cummins (1962) and Wehausen (1967), the time-domain ship motion can be solved directly by using the time-domain Green function derived by Finklestein (1957). The advantages of the direct method are that it can be extended to solve the quasi-nonlinear hydrodynamic problem as shown by Lin and Yue (1990). Moreover, it is easier to compute the time-domain Green function numerically than to compute the frequency-domain counterpart at forward speed. For the application of the three-dimensional time-domain Green function to the radiation and diffraction problems for ships with or without forward speed, see Beck and Liapis (1987), Beck and King (1989), and Lin and Yue (1994).

Lin and Yue (1990, 1994) report a recent study on the large-amplitude ship motions and sea loads in the time domain. The differences between Lin and Yue's work and the earlier work by others using the linear time-domain approximation are that, in the former, the wetted surface of the ship hull is re-panelized at each time step, and that the equations are established in the space-fixed coordinate system in order to make their method more adaptive. The free-surface condition is still a linearized one, so the time-domain Green function can be used.

In this work, linearized radiation and diffraction forces are assumed for the simulation of ship motion in waves. However, other forces, such as Froude-Krylov force, viscous damping force and maneuvering forces, are nonlinear. This approach might be less rigorous, but it was used in the capsize analysis (Huang et al., 1998), and provides satisfactory results.

It is almost impossible to directly solve the boundary-value problem of the radiation and diffraction potentials for a long-time simulation on a personal computer, because the computation of memory effects of wave and motion is very time-consuming. The impulse function method given by Cummins (1962) introduced an effective way to solve this cumbersome prob-

lem. Beck and King (1989) use the Fourier transform to obtain the impulse response functions of the radiated wave forces. However, the Fourier transform has to be cut off at a certain frequency to achieve convergent results. This method is not readily amenable to practical applications, because an appropriate cut-off frequency needs to be determined by numerical experiment for individual ships. In this work, the discretized Fredholm integral equation of the first kind for the response function is solved directly in the time domain at each instant. This method was found to be robust without much numerical difficulty.

2. NONLINEAR SHIP MOTION

Three coordinate systems used in our theoretical model are shown in Fig. 1.

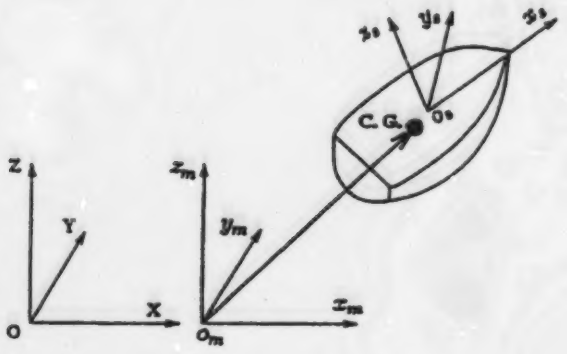

Fig. 1 Coordinate Systems for Ship Motions

Here, $OXYZ$ is the space-fixed coordinate system with the OXY plane on the calm-water surface and the OZ axis being positive upwards. The second coordinate system $o_m x_m y_m z_m$ is the equilibrium coordinate system that translates at the steady forward speed U of the ship in the OX direction maintaining the fixed orientation. At $t = 0$, the OXY system coincides with the $o_m x_m y_m z_m$ system. The third coordinate system $o_s x_s y_s z_s$ is fixed on the ship. The origin o_s of the body-fixed coordinate system coincides with o_m, and the $o_s x_s y_s$ plane coincides with the OXY plane when the ship is at its static equilibrium position, and the $o_s z_s$ axis is positive upwards. The ship is assumed to be rigid.

The oscillatory ship motions are described in the $o_m x_m y_m z_m$ system. The ship motions are represented by $(\xi_1, \xi_2, \xi_3, e_1, e_2, e_3)$, in which (ξ_1, ξ_2, ξ_3) are the displacements of the centre of gravity (CG), and (e_1, e_2, e_3) are the Eulerian angles of the ship in space. The Eulerian angles are the measurements of the ship's rotation about the axes which pass through the CG of the ship. The instantaneous translational velocities of ship motion in the directions of $o_s x_s$, $o_s y_s$ and $o_s z_s$ are u_1, u_2 and u_3, respectively, and the rotational velocities about axes parallel to $o_s x_s$, $o_s y_s$ and $o_s z_s$ and passing through the centre of gravity are u_4, u_5 and u_6, respectively. The equations of ship motion are:

$$[m_{kj}] \begin{pmatrix} \dot{u}_1 \\ \dot{u}_2 \\ \dot{u}_3 \\ \dot{u}_4 \\ \dot{u}_5 \\ \dot{u}_6 \end{pmatrix} + \begin{pmatrix} m\vec{\Omega} \times \vec{u} \\ \\ \vec{\Omega} \times ([I]\vec{\Omega}) \end{pmatrix} = \begin{pmatrix} F_1 \\ F_2 \\ F_3 \\ F_4 \\ F_5 \\ F_6 \end{pmatrix} \tag{1}$$

where $\vec{u} = (u_1, u_2, u_3)$, $\vec{\Omega} = (u_4, u_5, u_6)$, m is the ship mass, $[I]$ is the moment of inertia matrix, and $[m_{kj}]$ is the generalized mass matrix.

The total external forces on the ship are

$$F_k(t) = F_k^{Rs}(t) + F_k^{FK}(t) + F_k^{Dif}(t) + F_k^{Ra}(t) + F_k^{v}(t) + F_k^{H}(t) + F_k^{Rud}(t) \quad \text{for } k = 1, 2, \cdots, 6, \tag{2}$$

where F_k^{Rs} are the restoring forces; F_k^{FK} the nonlinear Froude-Krylov forces; F_k^{Dif} the diffracted wave forces; F_k^{Rad} the radiated wave forces; F_k^{v} the viscous forces including viscous roll damping moment and cross-flow drag; F_k^{H} the hull maneuvering forces; and F_k^{Rud} the rudder forces. The details of computing the hydrodynamic forces are presented in the technical report (Cong and Hsiung, 1998).

The ship's translational displacements (ξ_1, ξ_2, ξ_3) in the steady moving system and the Eulerian angles (e_1, e_2, e_3) are solved from:

$$\begin{pmatrix} \dot{\xi}_1 \\ \dot{\xi}_2 \\ \dot{\xi}_3 \\ \dot{e}_1 \\ \dot{e}_2 \\ \dot{e}_3 \end{pmatrix} = \begin{pmatrix} [R] & 0 \\ 0 & [B] \end{pmatrix} \begin{pmatrix} u_1 \\ u_2 \\ u_3 \\ u_4 \\ u_5 \\ u_6 \end{pmatrix} \tag{3}$$

where matrices $[B]$ and $[R]$ are defined as follows:

$$[B] = \begin{pmatrix} 1 & s_1 t_2 & c_1 t_2 \\ 0 & c_1 & -s_1 \\ 0 & s_1/c_2 & c_1/c_2 \end{pmatrix} \tag{4}$$

$$[R] = \begin{pmatrix} c_2 c_3 & s_1 s_2 c_3 - c_1 s_3 & c_1 s_2 c_3 + s_1 s_3 \\ c_2 s_3 & s_1 s_2 s_3 + c_1 c_3 & c_1 s_2 s_3 - s_1 c_3 \\ -s_2 & s_1 c_2 & c_1 c_2 \end{pmatrix} \tag{5}$$

and $c_i = \cos e_i$, $s_i = \sin e_i$, and $t_i = \tan e_i$ for $i = 1, 2, 3$.

Ship motions in the time domain are solved from twelve equations in (1) and (3). At each time step, the motion velocities in the ship-fixed coordinate system are obtained by integrating (1) with the velocities at the previous time step as the initial conditions. The ship motion displacements are solved from (3) in the steady moving coordinate system. The unknown ship motion at a new time step is required to compute the

motion at a new time step is required to compute the forces (e.g. the restoring force has to be calculated with the ship motion displacement). In this case, a linear prediction of stochastic theory is adopted to determine the ship motion for the force computation. Then, the ship motion is solved numerically from the first-order ordinary differential equations.

3. FORCES OF RADIATED AND DIFFRACTED WAVES

3.1 forces due to radiated waves

The impulse response function method is used to describe the radiation forces on the ship hull. This method was originally introduced by Cummins (1962) to discuss the radiation problem and to relate the time-domain hydrodynamic forces to those in the frequency domain. The radiation potential is caused not only by the oscillatory velocity but also by the oscillatory displacement which changes the position of the body in the steady flow field. The corresponding fluid motion can be separated into two parts: the impulsive motion and the subsequent wave motion.

During the impulsive motion, the ship is given an instantaneous displacement η_j in the j^{th} mode of motion, which can be considered to consist of a movement at the velocity $\dot{\eta}_j$ for a very small time interval Δt, and then the ship motion is terminated abruptly at the end of the time interval. At the same time, the free surface is elevated by a certain amount by the impulse velocity. After the impulse, this elevation will disperse and consequently cause motion of the fluid. Under the assumption that the fluid is inviscid and the flow is irrotational, the radiation potential ϕ_j can be written as:

$$\phi_j(P,t) = \dot{\eta}_j(t)\psi_j(P) + \eta_j(t)\chi_j(P) + \int_{-\infty}^{t} \varphi_j(P,t-\tau)\dot{\eta}_j(\tau)d\tau. \quad (6)$$

The boundary-value problems for potentials ψ_j, χ_j and φ_j at the point $P(X,Y,Z)$ are given in Appendix A. After the potential is found, the pressure on the hull and hence the hydrodynamic force due to the radiated waves corresponding to the impulsive motion can be obtained. In the time-domain analysis, the radiation force of the input motion is assumed to be linear. Hence, the method of response function of a linear system can be applied. Following the approach of Liapias and Beck (1985), the total radiation force is computed by

$$F_k^{Ra}(t) = \sum_{j=1}^{6} F_{kj}(t), \quad \text{for } k = 1,\ 2,\ ...,\ 6 \quad (7)$$

where the force F_{kj} can be obtained by integrating the pressure over the wetted hull surface, and finally,

$$F_{kj}(t) = -\bar{\mu}_{kj}\ddot{\eta}_j(t) - \bar{\lambda}_{kj}\dot{\eta}_j(t) - \bar{\gamma}_{kj}\eta_j(t) - \int_0^t K_{kj}(t-\tau)\dot{\eta}_j(\tau)d\tau. \quad (8)$$

In equation (8), the time-domain hydrodynamic, or added, mass of the ship is

$$\bar{\mu}_{kj} = \rho \int\int_S \psi_j n_k dS, \quad (9)$$

where $\vec{n} = (n_1, n_2, n_3)$ is the unit normal vector to the hull surface, pointing into the fluid.

The time-domain hydrodynamic damping coefficient is

$$\bar{\lambda}_{kj} = -\rho[\int\int_S \chi_j m_k dS - \int\int_S \psi_j n_k dS - \oint_\Gamma \psi_j n_k (\vec{l}\times\vec{n})\cdot\vec{\bar{W}}dl], \quad (10)$$

where $\vec{l}$ is the unit tangent vector to the mean waterline Γ.

The coefficient of the time-domain hydrodynamic restoring force is

$$\bar{\gamma}_{kj} = \rho[-\int\int_S \chi_j m_k dS - \oint_\Gamma \chi_j n_k (\vec{l}\times\vec{n})\cdot\vec{\bar{W}}dl], \quad (11)$$

where $\vec{\bar{W}}$ is the known velocity field around a ship due to the steady forward speed and m_k the so-called m-terms (see equations (40) and (41) below). The above hydrodynamic coefficients are computed in terms of the solutions of (47) and (48) in Appendix A. The response function, or kernel function, is given by

$$K_{kj}(t) = \rho[\int\int_S \frac{\partial\varphi_j(Q,t)}{\partial t} n_k dS - \int\int_S \varphi_j(Q,t) m_k dS - \oint_\Gamma n_k \varphi_j(Q,t)(\vec{l}\times\vec{n})\cdot\vec{\bar{W}}dl]. \quad (12)$$

One way to obtain the impulse response function is by introducing a non-impulsive input motion as follows (see e.g., Beck and King, 1989):

$$\dot{\eta}_j(t) = \sqrt{\frac{\bar{a}L}{\pi g}} e^{-\bar{a}t^2}. \quad (13)$$

Then the boundary condition on the body surface for the radiation problem becomes:

$$\frac{\partial\phi_j(P,t)}{\partial n_p} = \sqrt{\frac{\bar{a}L}{\pi g}} e^{-\bar{a}t^2} n_j + \frac{1}{2}\sqrt{\frac{L}{g}}\,\mathrm{erf}(\sqrt{\bar{a}}t) m_j. \quad (14)$$

where L is the ship length, and $\bar{a}$ is a constant ($\bar{a} = 0.1$ (s^{-2}) is used in this work). The source strength of the radiation potential can be found by substituting (14) into (53) in Appendix A. Since the non-impulse motion decays very fast, the computation for the radiated

waves is quite efficient. In this way, the radiation potential needs to be calculated only for a fraction of the total simulation time. This treatment makes it possible to carry out a long-time simulation of ship motions on a personal computer.

By using the potential function of the radiation waves expressed by (49) in Appendix A, the radiation force can be written as:

$$F_{ij}(t) = -\dot{g}_{ij}(t) - h_{ij}(t), \tag{15}$$

where

$$g_{ij}(t) = \rho \int\int_S \phi_j n_i dS, \tag{16}$$

$$h_{ij}(t) = -\rho \int\int_S \phi_j m_i dS - \rho \oint_\Gamma \phi_j (\vec{l} \times \vec{n}) \cdot \vec{W} n_i d\eta. \tag{17}$$

By equating (15) and (8), finally, we have

$$\int_0^t K_{ij}(t-\tau)\dot{\eta}_j(\tau)d\tau = f_{ij}(t) =$$
$$\dot{g}_{ij}(t) + h_{ij}(t) - \mu_{ij}\ddot{\eta}_j(t) - \lambda_{ij}\dot{\eta}_j(t) - \gamma_{ij}\eta_j(t) \tag{18}$$

Beck and King (1989) applied the Fourier transform to determine the response functions K_{ij}. The difficulty with their method is that the inverse Fourier transform has to be cut off at a certain frequency to have convergent results. The desirable cut-off frequency for a given mode varies for different hull forms and forward speeds, and can only be determined by numerical experiment.

In the present method, K_{ij} is determined by solving the integral equation (18) directly in the time domain; that is, by solving the following system of linear equations at each time step, such that,

$$\sum_{n=1}^{m-1}(K_{ij})_{m-n}(\eta_j)_n + \frac{1}{2}[(K_{ij})_m(\eta_j)_0 + (K_{ij})_0(\eta_j)_m] = \frac{(f_{ij})_m}{\Delta t} \tag{19}$$

where $m = 1, 2, ..., M$, M is the total number of time steps defined by $T = M\Delta t$, and T is the upper limit of the integration in equation (18).

The systems of equations (19) are indeterminate, because the total number of unknowns M is larger than the total number of equations by 1. In this work, an additional condition is derived from physical consideration as follows:

$$(K_{ij})_{N-1} - 2(K_{ij})_N + (K_{ij})_{N+1} = 0 \tag{20}$$

where N is an arbitrary number. In choosing an optimum value for N, we note that the response function $(K_{ij})_m$ becomes quite smooth after a sufficiently long time, $t_m = m\Delta t$, and asymptotically goes to zero. According to our experience, setting N to a value between $M/2$ and $3M/4$ will result in a stable solution.

The method has been tested for several floating bodies. Sample results are presented in this paper. Fig. 2 shows the computed response function $K_{33}(t)$ for a hemi-sphere of radius $R = 5$ m compared with Barakat's result (1962). By using the response function $K_{33}(t)$ and the Fourier transformation, the corresponding added mass and damping coefficients in the frequency domain can be found (Liapis and Beck, 1985). Fig. 3 shows the comparison of the present results with Barakat's results. Similarly, the function $K_{33}(t)$ for the ship hull Series 60 ($C_b = 0.7$) compared with Liapis's computation is shown in Fig. 4, and the comparisons of added mass and damping coefficients are shown in Fig. 5.

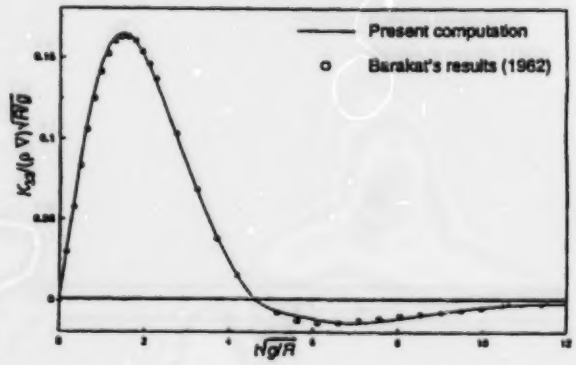

Fig. 2 Response function $K_{33}(t)$ of a hemisphere ($F_n = 0$)

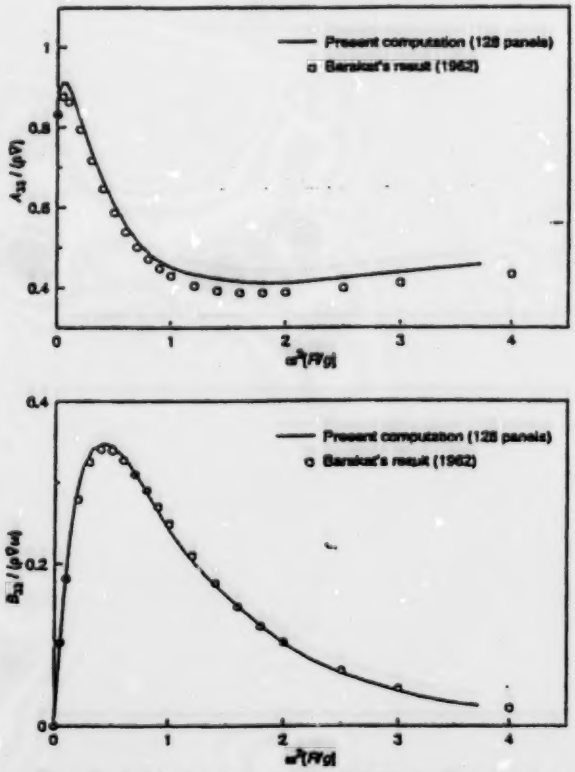

Fig. 3 Added mass and damping coefficient of a hemisphere ($F_n = 0$)

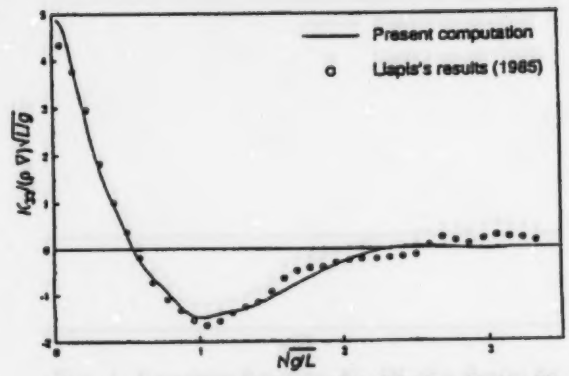

Fig. 4 Response function $K_{33}(t)$ of a Series 60 $C_b = 0.7$ ($F_n = 0$)

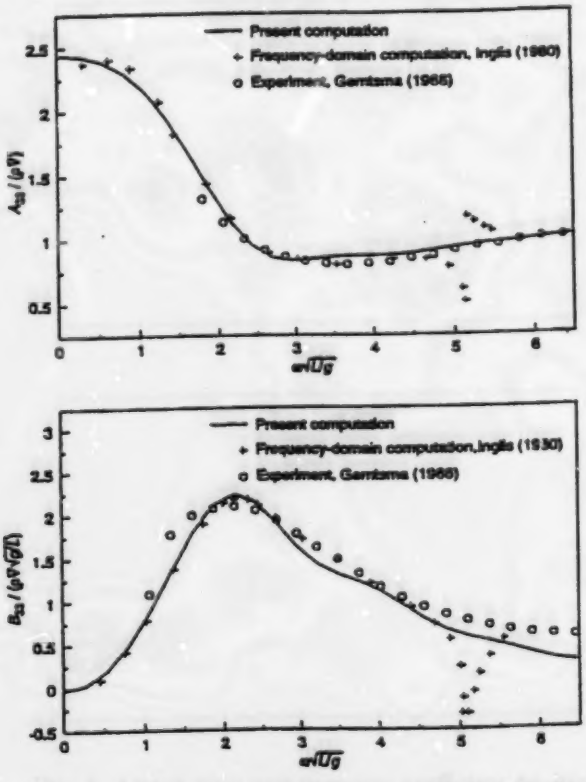

Fig. 5 Added mass and damping coefficient for Series 60 $C_b = 0.7$ ($F_n = 0$)

3.2 forces due to diffracted waves

The time history of free-surface elevation of irregular waves can be represented by the superposition of sinusoidal waves of all frequencies with random phases. For a given wave spectrum $S_{\zeta\zeta}(\omega)$, the wave elevation is expressed as below:

$$\zeta_i(X,Y,t) = \sum_{j=1}^{\infty} \zeta_a(\omega_j)\cos(k_j X\cos\beta + k_j Y\sin\beta - \omega_j t + \varepsilon_j), \qquad (21)$$

where

$$\zeta_a(\omega_j) = \sqrt{2S_{\zeta\zeta}(\omega_j)(\omega_j - \omega_{j-1})} \qquad (22)$$

is the amplitude of the jth component wave, the random phase angle ε_j has a uniform distribution over $[0, 2\pi)$. The wave number is $k_j = \omega_j^2/g$, where ω_j is the angular frequency, and β is the wave heading angle. In the manner similar to that for the radiated waves, the forces of diffracted waves can be written as:

$$F_{i7}(t) = \int_{-\infty}^{t} K_{i7}(t-\tau)\zeta_0(\tau)d\tau, \qquad (23)$$

where $\zeta_0(\tau)$ is the free surface elevation of incident waves at the origin o_s of the moving coordinate system, and K_{i7} is the response function for the i^{th} mode diffraction force. Before the incident waves arrive at o_s, they have touched the ship hull first, and so K_{i7} is not zero for $t < 0$. Therefore the lower limit of the integral in (23) is $-\infty$ rather than 0. Once the response function K_{i7} is solved, the diffraction force can be computed by using equation (23).

In order to obtain the response function $K_{i7}(t)$, the following non-impulsive incident wave at the origin o_s of the body-fixed coordinate system was used (Beck and King, 1989) in this work.

$$\zeta_0(t) = \frac{1}{\pi} Re\{\int_0^{\infty} e^{-\omega^2/4\pi} e^{i\omega_e t} d\omega_e\}. \qquad (24)$$

After the diffraction potential ϕ_7 is obtained, the force due to the diffracted waves can be expressed as:

$$F_{i7}(t) = -\dot{g}_{i7}(t) - h_{i7}(t), \qquad (25)$$

where

$$g_{i7}(t) = \rho \int\int_S \phi_7 n_i dS, \qquad (26)$$

and

$$h_{i7}(t) = -\rho \int\int_S \phi_7 m_i dS - \rho \oint_\Gamma \phi_7 (\vec{l}\times\vec{n})\cdot\bar{\bar{W}} n_i dl. \qquad (27)$$

Letting (23) equal to (25), we have

$$\int_{-\infty}^{t} K_{i7}(t-\tau)\zeta_0(\tau)d\tau = -\dot{g}_{i7}(t) - h_{i7}(t). \qquad (28)$$

The above equation is similar to (18). The only difference here is that the integration interval is $(-\infty, t)$, not $(0, t)$ as in the case of radiated waves. Hence, the response function K_{i7} can be solved with the same numerical scheme, namely the method of direct solution.

The computed response functions, $K_{27}(t)$ and $K_{37}(t)$, for a hemi-sphere of radius 5 m are compared with Beck and King's results (1989) in Fig. 6.

In the present method, hydrodynamic forces are expressed as the convolution products of a response kernel with either the velocity of ship motion in a given mode or the wave elevation. For example, the convolution kernels for the radiation forces are obtained for each

of the six modes of motion by numerically solving the Fredholm integral equation of the first kind. The radiation response function K_{ij} needs to be solved only for a relatively short period of time for the impulsive input motion. The computation of response functions of radiated and diffracted waves were designed as two independent modules in the present work. Once these two modules are run, the Green function does not need to be evaluated in the process of solving the equations of ship motion. Thus, the most time-consuming calculations of the time-domain Green function need to be done only for a relatively short period of time.

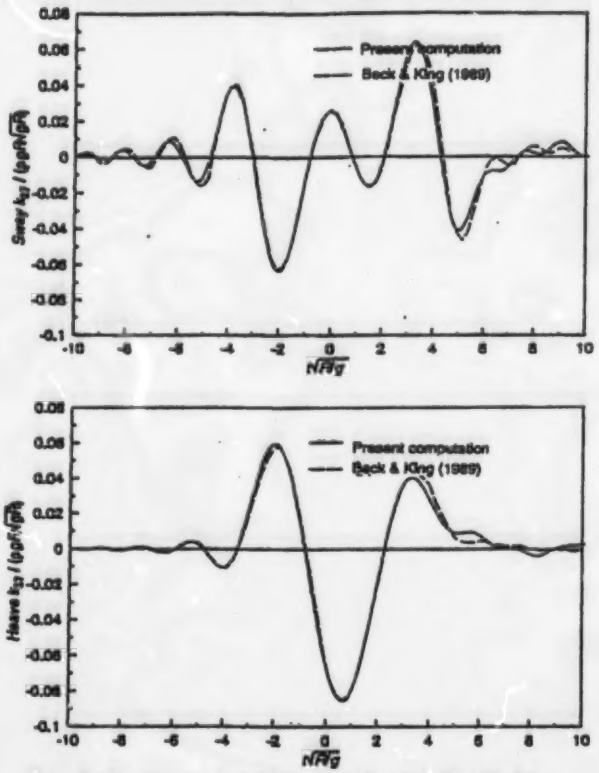

Fig. 6 Response function $K_{27}(t)$ and $K_{37}(t)$ for a hemisphere ($F_n = 0$)

4. PRESSURE ON HULL

The total hydrodynamic pressure p_t on the hull surface can be decomposed as follows:

$$p_t(P,t) = p_o(P,t) + p_r(P,t) + p_d(P,t) \qquad (29)$$

where $p_o(P,t)$ is the pressure due to incident waves, $p_r(P,t)$ the pressure due to radiated waves, and $p_d(P,t)$, the pressure due to diffracted waves.

In an incident wave field, the wave profile $\zeta_o(X,Y,t)$ can be computed at all nodal points on the ship hull. The vertical coordinate Z of nodal points on the wetted hull surface is compared with the incident wave surface. If a nodal point is below the wave surface $\zeta_o(X,Y,t)$, then the nonlinear pressure due to the incident wave is computed by:

$$p_o(P,t) = -\rho g[Z - \zeta_i(P,t)] - \rho\frac{\partial\Phi_i(P,t)}{\partial t} - \frac{1}{2}\rho|\nabla\Phi_i(P,t)|^2 \qquad (30)$$

As mentioned in the last section, the time series of potentials of radiated and diffracted waves are not computed in the present method; instead, the forces due to the radiated and diffracted waves are computed by the response functions. The same approach can be adopted for the computation of the pressure due to the radiated and diffracted waves.

The pressure of radiated waves due to all modes of motion is computed by:

$$p_r(P,t) = \sum_{j=1}^{6} p_{rj}(P,t). \qquad (31)$$

Under the linearity assumption, the relationship between the output pressure $p_{rj}(P,t)$ and the input motion $\dot{\eta}_j(t)$ can be written as:

$$p_{r_j}(P,t) = \int_0^t K_{pr_j}(P,t-\tau)\dot{\eta}_j(\tau)d\tau \qquad (32)$$

The same solution method as used for (18), i.e. equations (19) and (20), can be used to solve this Fredholm integral equation for $K_{pr_j}(P,t)$. To this end, the radiation potential ϕ_j and its partial derivatives induced by the j^{th} mode of motion $\eta_j(t)$ are first soived. Then the radiation pressure $p_{r_j}(P,t)$ on the left-hand side of (32) is computed by:

$$p_{r_j}(P,t) = -\rho\frac{\partial\phi_j}{\partial t} - \rho\vec{W}\cdot\nabla\phi_j. \qquad (33)$$

Equation (32) is to be solved at each panel point to obtain the pressure distribution on the hull.

Similar to solving for $K_{pr_j}(P,t)$ from equation (32), the response function of diffraction pressure $K_{pd}(P,t)$ can be solved from

$$p_d(P,t) = \int_{-\infty}^{\infty} K_{pd}(P,t-\tau)\zeta_0(\tau)d\tau. \qquad (34)$$

From the response functions K_{pr_j} and K_{pd}, the ship motion $\dot{\eta}_j(t)$, and the incident wave at the origin, $\zeta_0(t)$, the pressure distribution due to radiated and diffracted waves can be computed by equations (31), (32), and (34). Finally, the total pressure can be obtained, by adding the pressure of incident waves (30).

Once we have obtained the hydrodynamic forces on the ship hull and the ship motion in the time domain, it is straight forward to compute the sea loads. Sea loads consist of two parts: one is the static load which is the difference between the weight distribution and

the buoyancy distribution of the ship at the rest position in calm water; and the other part is the dynamic sea load which is due to body inertial forces, restoring forces and hydrodynamic forces. In the time-domain simulation, we are only interested in the dynamic sea load. The vertical shear force F_S and the vertical bending moment M_B for a cross section at $x = x_c$ are given by:

$$\begin{aligned} F_S &= F_I + F_P \\ M_B &= M_I + M_P \end{aligned} \tag{35}$$

where, F_I and M_I are inertial force components, acting on the cross section at x_c, F_P and M_P are forces including all other hydrodynamic components, i.e. the restoring and Froude-Krylov forces, radiation and diffraction forces. This hydrodynamic component of sea loads can be computed by the direct integration of the pressure over the hull portion forward of x_c. Impact loads are not included in this work.

The inertial force components are computed as follows:

$$\begin{aligned} F_I &= m_{cx}\dot{u}_3 - m_{cx}(x_g - x_G)\dot{u}_5 \\ M_I &= m_{cx}(x_g - x_c)\dot{u}_3 - m_{cx}r_{xx}[r_{xx} - (x_c - x_G)]\dot{u}_5 \end{aligned} \tag{36}$$

where m_{cx} is the mass of the portion of the ship between the bow and the cross section x_c, x_g and x_G are the x coordinates of the centres of gravity of the ship segment forward of x_c and of the whole ship, respectively; and r_{xx} is the radius of gyration of the portion of the ship forward of x_c.

At each time step, the wetted panels on the hull forward of x_c are selected based on the ship displacement and the incident wave profile. After all components of hydrodynamic pressures are computed in terms of equation (29) on the whole hull surface, the sea loads due to the hydrodynamic pressure can be calculated by the direct integration of the pressure over the hull portion between bow and x_c:

$$\begin{aligned} F_P(t) &= \int_{S_F} p_t(P,t) n_3 dS \\ M_P(t) &= \int_{S_F} p_t(P,t) n_3 (x_p - x_c) dS \end{aligned} \tag{37}$$

where S_F is the surface of the hull between the bow and the cross section at x_c, n_3 is the z component of the normal vector, while x_p is the x coordinate of the hull point P.

5 NUMERICAL RESULTS

The proposed method has been used to compute the motions, pressures and sea loads of a frigate with a steady forward speed in regular head waves. The half-hull under the mean waterline is panelized into 153 panels. Some numerical results given below are corresponding to the following conditions:

ship speed: V_s=3.4 knots (Froude number 0.05);
wave steepness: H/λ=1/50;
ratio of wave and ship lengths: λ/L=1.19;
where H is the wave height, λ is the wave length, and the ship length L=124.5 m.

The input wave and the predicted heave and pitch of the ship by the present method are shown in Fig. 7. The predicted and measured phase angles for both motions are in good agreement. The heave downward motion, however, is underestimated, while the pitch amplitudes are somewhat overestimated. These apparent deficiencies are being addressed in the on-going work to improve the code.

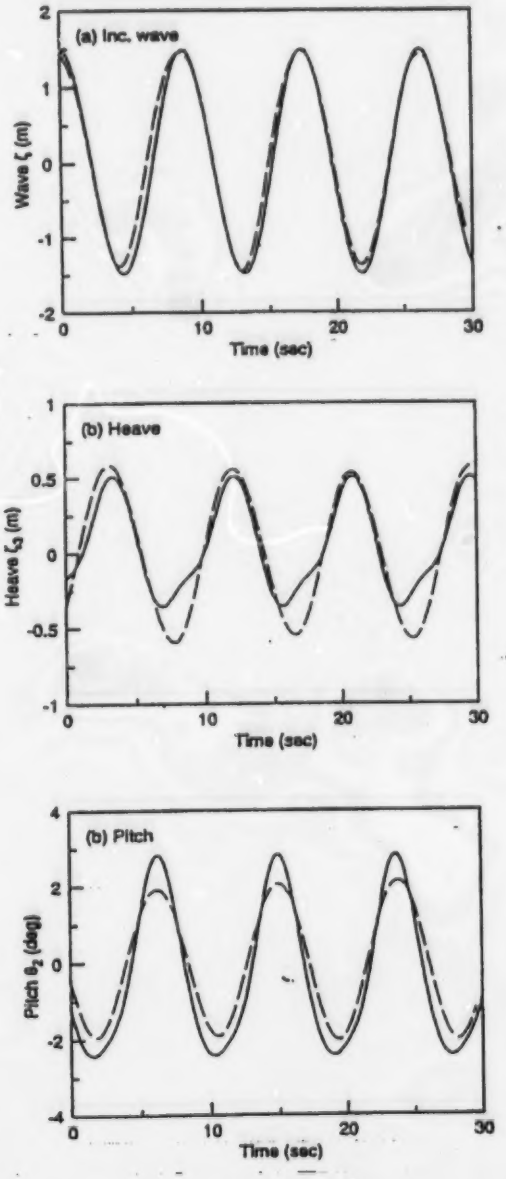

Fig. 7 Wave elevation and motions of the frigate (— the prediction; - - - experiment).

Examples of comparisons between the computed and measured pressures are shown in Fig. 8. The discrepancy is rather large at station 1, which is near the ship bow. This may be indicative of nonlinearity in the flow around the ship bow, which was neglected in this theoretical model; see e.g. Ando and Cumming (1991). Figure 9 shows the comparison of the vertical shear force and bending moment amidships.

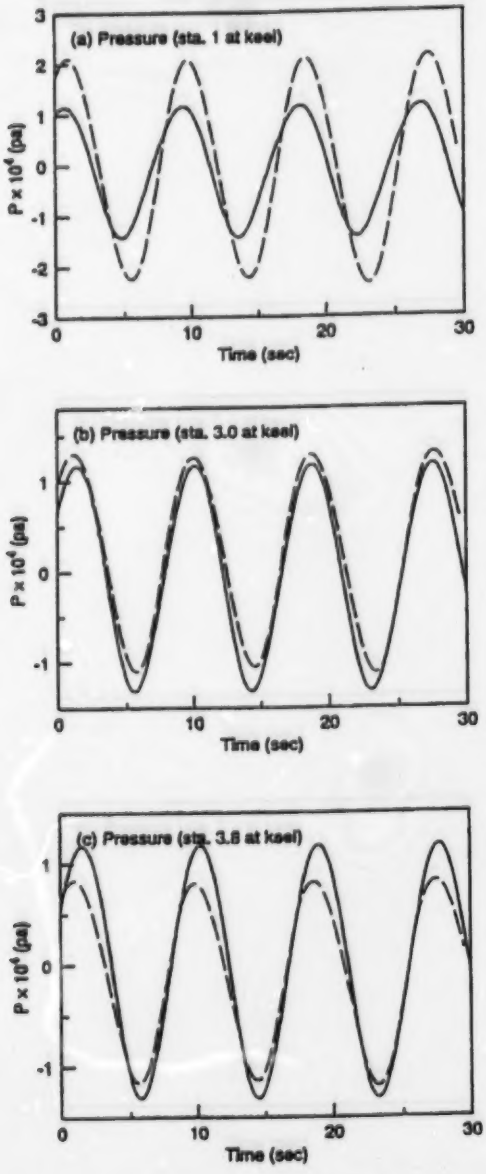
(a) Pressure (sta. 1 at keel)
P x 10⁴ (pa)
Time (sec)
(b) Pressure (sta. 3.0 at keel)
P x 10⁴ (pa)
Time (sec)
(c) Pressure (sta. 3.8 at keel)
P x 10⁴ (pa)
Time (sec)

Fig. 8 Hull pressure on the frigate
(— the prediction; - - - experiment).

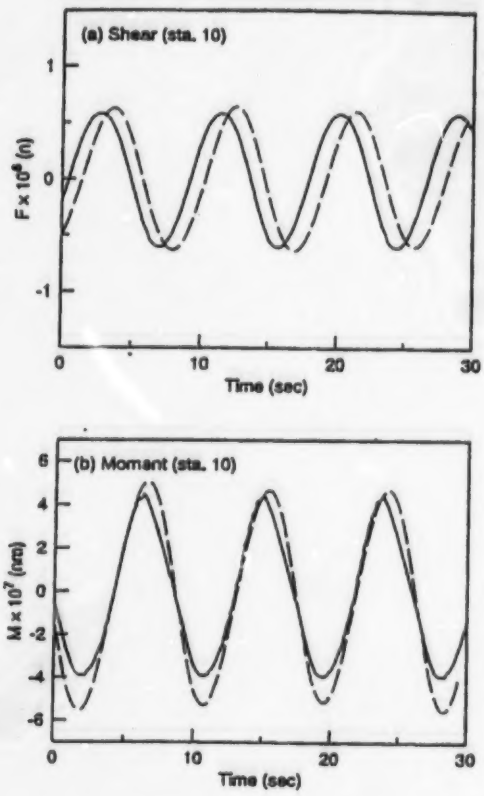

Fig. 9. Sea loads for the frigate
(— the prediction; - - - experiment).

CONCLUSION

In this work, a methodology for predicting ship motions, hydrodynamic pressure and sea loads in waves has been developed. Nonlinear effects of the ship motions in large amplitude waves are considered in the Froude-Krylov forces, roll damping forces, cross-flow drag, manoeuvring forces and rudder forces. The linear assumption is applied to the forces due to the radiated and diffracted waves. The nonlinear ship motions are solved in the time domain.

In this work, the Fredholm integral equations of the first kind for the impulse response functions for the radiated and diffracted waves were solved directly in the time domain. By this method, we were able to successfully overcome the numerical difficulties that would attend the commonly used Fourier transformation method. Separate response functions for the forces and pressures were derived for both radiated and diffracted waves. By the present approach, the computational demand of the time-domain simulation of ship motions and hull pressure distributions was significantly reduced, so that a personal computer could be used. Nonlinear sea loads were computed by the direct surface integration of the hydrodynamic pressure

distribution on the ship hull.

Generally speaking, the agreement between computed and experimental results was promising. The work to improve the code is on-going. Further validation will be carried out for different wave conditions and ship speeds.

REFERENCES

Ando, S. and Cumming, D.C., 1991, "Head-Wave Diffraction by a Slender Ship", *International Shipbuilding Progress*, Vol. 38, No. 414, pp.99-113.

Barakat, R., 1962, "Vertical Motion of the Floating Sphere in a Sine-Wave Sea", *Journal of Fluid Mechanics*, Vol. 13, pp.540-556

Beck, R. F. and King, B., 1989, "Time-Domain Analysis of Wave Exciting Forces on Floating Bodies at Zero Forward Speed", *Applied Ocean Research*, Vol. 11, pp.19-25

Beck, R. F. and Liapis, S. J., 1987, "Transient Motion of Floating Bodies at Zero Forward Speed", *Journal of Ship Research*, Vol. 31, pp.164-176

Cong. L. Z. and Hsiung C. C., 1998, "Development of Three-Dimensional Nonlinear Time-Domain Sealoads Computer Code", *Technical Report*, Centre for Marine Vessel Development and Research, DalTech, Dalhousie University, Canada.

Cummins, W. E., 1962, "The Impulse Response Function and Ship Motions", *Schiffstechnik*, Vol. 9, pp.101-109

de Kat, Jan O. and Paulling, J. R., 1989, "The Simulation of Ship Motions and Capsizing in Severe Seas", *Transactions of SNAME*, Vol. 97, pp.139-168

Finklestein, A., 1957, "The Initial Value Problem for Transient Water Waves", *Communications on Pure and Applied Mathematics*, Vol. 10, pp.511-522

Gerritsma, J., 1966, "Distribution of Hydrodynamic Forces along the Length of a Ship Model in Waves", *Report No. 144*, Ship Building Laboratory, Technological University of Delft, Delft, Netherlands.

Huang Z. J., Cong L. Z., Grochowalski S. and Hsiung C. C., 1998, "Capsize Analysis for Ships with Water Shipping on and off the Deck", *Proceedings of the 22nd Symposium on Naval Hydrodynamics*, Washington, D.C., USA

Huang, Z. J. and Hsiung, C. C., 1991, "A New Algorithm for the Three-Dimensional Time -Domain Green Function", *Technical Report NA-91-2*, Department of Mechanical Engineering, Technical University of Nova Scotia

Huang, Z. J. and Hsiung, C. C., 1997, "Dynamic Simulation of Capsizing for Fishing Vessels with Water on Deck", *STAB'97*, Varna, Bulgaria.

Inglis, R. B., 1980, "A Three-Dimensional Analysis of the Motion of a Rigid Ship in Waves", *Ph. D. Thesis*, Department of Mechanical Engineering, University College, London.

Liapis, S. and Beck, R. F., 1985, "Seakeeping Computations Using Time Domain Analysis", *Proceedings of the Fourth International Conference on Numerical Ship Hydrodynamics*, Washington, D.C.

Lin, W. M. and Yue, D. K., 1990, "Numerical Simulations for Large Amplitude Ship Motions in the Time Domain", *Proceedings of the 18th Symposium on Naval Hydrodynamics*, Ann Arbor, Michigan

Lin, W. M. and Yue, D. K., 1994, "Large Amplitude Motions and Wave Loads for Ship Design", *Proceedings of the 20th Symposium on Naval Hydrodynamics*, Santa Barbara, California

Wehausen J. V., 1967, "Initial Value Problem for the Motion in an Undulating Sea of a Body with Fixed Equilibrium Position", *Journal of Engineering Mathematics*, Vol. 1, pp.1-19

APPENDIX A: POTENTIAL OF RADIATED WAVES

For a ship undergoing a small-amplitude motion $\eta_j(t)$ in the j^{th} mode, the potential of the radiated waves is given by (see, Liapis and Beck, 1985),

$$\phi_j(P,t) = \dot{\eta}_j(t)\psi_j(P) + \eta_j(t)\chi_j(P) + \int_{-\infty}^{t} \varphi_j(P, t-\tau)\dot{\eta}_j(\tau)d\tau. \tag{38}$$

It can be shown that $\phi_j(P,t)$ at the location $P(X,Y,Z)$ should satisfy the Laplace equation subject to the boundary conditions at the free surface, the hull surface and the far field. The initial condition should also be specified.

Then, the time-independent velocity potential ψ_j satisfies the following conditions:

$$\begin{cases} \nabla^2\psi_j = 0 \\ \psi_j = 0 \quad \text{on} \quad z_m = 0, \\ \frac{\partial\psi_j}{\partial n} = n_j \quad \text{on} \quad \bar{S}, \\ \nabla\psi_j \to 0 \quad \text{as} \quad R \to \infty \quad \text{on} \quad z_m = 0, \\ \nabla\psi_j \to 0 \quad \text{as} \quad z_m \to -\infty. \end{cases} \tag{39}$$

where $\bar{S}$ is the mean wetted surface of the ship hull, and $R = \sqrt{x_m^2 + y_m^2}$.

The potential function χ_j, which is due to the displacement of ship motion in the steady flow field, satisfies an equation similar to (39), except that the hull surface condition becomes:

$$\frac{\partial\chi_j}{\partial n} = m_j \quad \text{on} \quad \bar{S}, \tag{40}$$

where m_j are the so-called m-terms, defined by:

$$(m_1, m_2, m_3) = -(\vec{n} \cdot \nabla)\vec{W},$$
$$(m_4, m_5, m_6) = -(\vec{n} \cdot \nabla)(\vec{r} \times \vec{W}), \tag{41}$$

and r is the position vector relative to o_s. During the impulsive phase, the free surface is elevated by an amount

$$\Delta\zeta_j = (\eta_j \frac{\partial \psi_j}{\partial z_m} + \eta_j \frac{\partial \chi_j}{\partial z_m})\Delta t. \tag{42}$$

After the impulse, this elevation will disperse and consequently causes the motion of the fluid. The corresponding velocity potential, $\varphi(P,t)$, which is referred to as the wave-induced potential, is proportional to the motion of the ship.

By Green's theorem, the potentials can be expressed by source strength distributions:

$$\chi_j(P) = -\frac{1}{4\pi}\int\int_S \sigma_j^{\chi}(Q)(\frac{1}{r} - \frac{1}{r_1})dS \tag{43}$$

and

$$\psi_j(P) = -\frac{1}{4\pi}\int\int_S \sigma_j^{\psi}(Q)(\frac{1}{r} - \frac{1}{r_1})dS \tag{44}$$

where

$$r^2 = (X-\xi_0)^2 + (Y-\eta_0)^2 + (Z-\zeta_0)^2 \tag{45}$$

$$r_1^2 = (X-\xi_0)^2 + (Y-\eta_0)^2 + (Z+\zeta_0)^2 \tag{46}$$

Using the boundary condition on the body surface, the values of the source strength ψ_j and χ_j can be determined from the following integral equations:

$$-\frac{\sigma_j^{\chi}(P)}{2} - \frac{1}{4\pi}\int\int_S \sigma_j^{\chi}(Q)\frac{\partial}{\partial n_P}(\frac{1}{r} - \frac{1}{r_1})dS = n_j(P) \tag{47}$$

and

$$-\frac{\sigma_j^{\psi}(P)}{2} - \frac{1}{4\pi}\int\int_S \sigma_j^{\psi}(Q)\frac{\partial}{\partial n_P}(\frac{1}{r} - \frac{1}{r_1})dS = m_j(P). \tag{48}$$

Since potentials ψ_j and χ_j are independent of time, equations (47) and (48) need to be solved only once before solving for the motions.

In cases where the impulsive input motion is not used, the potential function of the radiated waves can be expressed as:

$$\phi_j(P,t) = \frac{-1}{4\pi}\int_0^t d\tau \int\int_S \sigma_j(Q,\tau)G(P,Q,t-\tau)dS - \frac{U^2}{4\pi g}\int_0^t d\tau \oint_\Gamma n_1\sigma_j(Q,\tau)G(P,Q,t-\tau)dl \tag{49}$$

Here, G is the time-domain Green function:

$$G(P,Q,t) = G_0(P,Q)\delta(t) + G_f(P,Q,t)H(t) \tag{50}$$

where $P = (X,Y,Z)$ is the field point and $Q = (\xi_0, \eta_0, \zeta_0)$ is the source point in the $OXYZ$ system, $H(t)$ is the unit step function ($H(t) = 0$ for $t < 0$ and $H(t) = 1$ for $t > 0$), and

$$G_0(P,Q) = \frac{1}{r} - \frac{1}{r_1}, \tag{51}$$

$$G_f(P,Q,t) = 2\int_0^\infty dk\sqrt{gk}\sin[\sqrt{gk}t]e^{k(z+\zeta)}J_0(kR) \tag{52}$$

where J_0 is the Bessel function of the first kind of order zero. In this work, the method of computation of the Green function proposed by Huang and Hsiung (1991) has been refined to further speed up the simulation.

Then, the boundary condition on the body surface for the radiation potential is expressed as follows:

$$\frac{\partial \phi_j(P,t)}{\partial n_P} = -\frac{\sigma_j(P,t)}{2} - \frac{1}{4\pi}\int_0^t d\tau \int\int_S \sigma_j(Q,\tau)\frac{\partial G(P,Q,t-\tau)}{\partial n_P}dS \tag{53}$$

The numerical scheme to solve the potential functions from (53) is given in Appendix B.

APPENDIX B: NUMERICAL SCHEME TO SOLVE RADIATION POTENTIAL

The discretized Green function can be written as

$$G_{ij}^{k_t - k_\tau} = G_{0ij}\delta[(k_t - k_\tau)\Delta t] + G_{fij}^{k_t - k_\tau}H[(k_t - k_\tau)\Delta t] \tag{54}$$

where the current time instant $t = k_t\Delta t$, or $\tau = k_\tau\Delta t$, is the time variable in the convolution product in equation (53). In the subscripts, 0 refers to the Rankine source and its image, f the wave part, i the field point, and j the source point. In equation (54),

$$G_{0ij} = \frac{1}{r_{ij}} - \frac{1}{r_{1ij}} \tag{55}$$

$$G_{fij}^{k_t - k_\tau} = 2\int_0^\infty \sqrt{gk}\sin[\sqrt{gk}(k_t - k_\tau)\Delta t] e^{k(z_i+\zeta_j)}J_0(kR_{ij})dk \tag{56}$$

where

$$R_{ij} = \sqrt{(x_i-\xi_j)^2 + (y_i-\eta_j)^2} \tag{57}$$

$$r_{ij} = \sqrt{(x_i-\xi_j)^2 + (y_i-\eta_j)^2 + (z_i-\zeta_j)^2} \tag{58}$$

$$r_{1ij} = \sqrt{(x_i-\xi_j)^2 + (y_i-\eta_j)^2 + (z_i+\zeta_j)^2} \tag{59}$$

Under the assumption that the source strength on each panel is constant, the integral equations for the

potential of radiated waves can be discretized as follows:

$$-\frac{1}{2}(\sigma_J)_i^{k_t} + \sum_{j=1}^{N_p}(\sigma_J)_i^{k_t} I_{s0ij}$$
$$+\Delta t[\frac{1}{2}\sum_{j=1}^{N_p}(\sigma_J)_j^0 I_{sfij}^{k_t} + \sum_{k_\tau=1}^{k_t-1}\sum_{j=1}^{N_p}(\sigma_J)_j^{k_\tau} I_{sfij}^{k_t-k_\tau}]$$
$$= \sqrt{\frac{\bar{a}L}{\pi g}}e^{-\bar{a}(k_t\Delta t)^2}(n_J)_i - \frac{1}{2}\sqrt{\frac{L}{g}}\mathrm{erf}(\sqrt{\bar{a}}t)(m_J)_i \quad (60)$$

where $J = 1, 2, \cdots, 6$ are the modes of motion of the body, and the integration on a panel,

$$\begin{cases} I_{s0ij} = -\frac{1}{4\pi}\int\int_{\Delta S_j}(\frac{\partial G_0}{\partial n})_{ij}dS \\ I_{sfij}^{k_t-k} = -\frac{1}{4\pi}\int\int_{\Delta S_j}(\frac{\partial G_f}{\partial n})_{ij}^{k_t-k}dS \end{cases} \quad (61)$$

Since $G_{fij}^{k_\tau-k_t} = 0$ when $k_\tau = k_t$, a system of linear algebraic equations can be derived as:

$$\sum_{j=1}^{N_p} A_{ij}^{k_t}(\sigma_J)_j^{k_t} = B_i^{k_t} \quad i = 1\cdots N_p \quad (62)$$

where

$$A_{ij}^{k_t} = -\frac{1}{2}\delta(i-j) + I_{s0ij} \quad (63)$$

and

$$B_i^{k_t} = b_i^{k_t} - \Delta t[\frac{1}{2}\sum_{j=1}^{N_p}(\sigma_J)_j^0 I_{sfij}^{k_t} + \sum_{k=1}^{k_t-1}\sum_{j=1}^{N_p}(\sigma_J)_j^k I_{sfij}^{k_t-k}] \quad (64)$$

and

$$b_i^{k_t} = \sqrt{\frac{\bar{a}L}{\pi g}}e^{-\bar{a}(k_t\Delta t)^2}(n_J)_i - \frac{1}{2}\sqrt{\frac{L}{g}}\mathrm{erf}(\sqrt{\bar{a}}k_t\Delta t)](m_J)_i \quad (65)$$

The two-dimensional Gaussian quadrature is used to compute the numerical integral on a panel for equation (61).